Austin Chemical Engineering

Austin Publishing Group

Open Access Full Text Article

Review Article

CO Oxidation by Cobalt Oxide: An Experimental Study on the Relationship between Nanoparticle Size and Reaction Kinetics

Bijith D Mankidy, Nianthrini Balakrishnan, Babu Joseph* and Vinay K Gupta

Department of Chemical & Biomedical Engineering, University of South Florida, USA

***Corresponding author:** Babu Joseph, Department of Chemical & Biomedical Engineering, University of South Florida, ENB 118, 4202 E Fowler Ave, Tampa, FL 33620, USA

Received: July 11, 2014; **Accepted:** Aug 04, 2014; **Published:** Aug 07, 2014

Abstract

CoO nanoparticles of different sizes (1-14nm) were synthesized using colloidal techniques. Nanoparticle size was controlled by adjusting the ratio of cobalt precursor to surfactant. Activation energies for CO oxidation as a function of nanoparticle size were experimentally measured in an in-situ FTIR reactor using transient state kinetic studies. Experimental results are in agreement with a two-step mechanism for CO oxidation: CO reacts with O2 to form an intermediate OCO followed by the dissociation of the intermediate to CO2 molecule. The activation energies for CO oxidation reaction increased as the size of CoO nanoparticle increased. Experimental measurements of activation energy vary from 9.4kJ/mol to 21.3kJ/mol for step-1 and from 63.6kJ/mol to 95.4kJ/mol for step-2 as the size of CoO nanoparticle increases. The findings reported here shed light on the size effect and mechanistic aspects of CO oxidation on CoO.

Keywords: CO Oxidation; CoO Nanoparticle; Size-effect; In-situ FTIR

Introduction

The use of nanometer sized catalysts has been of widespread interest as the nanoscale provides several advantages. Nanoparticle catalysts possess an increased number of active sites per unit mass of catalyst material, which helps to reduce the amount of catalyst especially when the catalyst material used is expensive. In addition, as the size of nanoparticle decreases, the percentage of atoms on the surface with low coordination number increases [1], which enhances the effect associated to corners or edges of a nanoparticle that possess unique electronic properties compared to an atom on a flat surface. For example, studies by Dahl and coworkers [2] on single crystal ruthenium, Ru(001) have shown high activity of N_2 molecule on edge sites with lower coordination numbers compared to atoms on a flat surface that possess higher coordination numbers. In the study, Dahl and coworkers used experiments and DFT calculations to demonstrate that dissociation of N_2 on step sites was at least 9 orders of magnitude higher than on terraces [2].

In a similar manner, the chemistry of different reactions may be tuned by using nanoparticles of different sizes. For example, CO oxidation is an important reaction from a scientific and an industrial point of view due to the interest in purification of indoor air and automotive or industrial exhausts, and in the production of H_2 rich feed streams devoid of CO for the fuel cell industry [3-7]. In the case of CO oxidation reaction, gold and other noble metals such as Pt, Ru, Rh, Ir have been extensively studied and the role of catalyst size on the reaction kinetics has been well established. Recently, there have been a few reports on inexpensive non-noble metal catalysts for CO oxidation.[4,8-14] For instance, Xie and coworkers [15] have synthesized unique nanorod-shaped catalysts using cobalt oxide (Co_3O_4) that oxidize CO at temperatures as low as -77°C. The author describes that this behavior may be due to the higher chemical activity of preferentially exposed atoms on the catalyst surfaces of the nanorods.

These past reports underscore the importance of morphology of base transition metal oxides and of understanding the role of these unique structural features to develop highly efficient oxidation catalysts. To the best of our knowledge, systematic understandings of the impact of CoO nanoparticle size using experiments are limited. To understand the effect of size on CO oxidation, we synthesized CoO nanoparticles of different sizes and systematically examined CO oxidation as a function of nanoparticle size using in-situ FTIR studies. Activation energies of reaction steps were measured experimentally using in-situ FTIR studies under transient conditions to gain insight into the reaction mechanisms [16, 17]. Experimental results suggest that CO oxidizes via a two-step mechanism: CO reacts with O_2 to form an intermediate OCO followed by the dissociation of the intermediate to CO_2 molecule. The activation energies for CO oxidation reaction increased as the size of CoO nanoparticle increased.

Prior studies suggest 3 possible mechanisms for CO oxidation on metal and metal oxide surfaces: [15,18,19]

I. $CO + O_L \rightarrow CO_2 + O_V$

II. $CO + O_2 \rightarrow OOCO \rightarrow CO_2 + O$

III. $CO + O_2 \rightarrow O + OCO \rightarrow CO_2 + O$

In Mechanism I, CO adsorbed on the surface reacts with the lattice oxygen O_L on the CoO(100) surface to form CO_2 and leaves a vacant oxygen site (O_V) on the surface [15]. In Mechanism II, CO adsorbed on the surface reacts with adsorbed oxygen to form an intermediate OOCO which later forms CO_2 leaving an oxygen atom behind on the surface [19]. In Mechanism III, CO adsorbed on the

Citation: Mankidy BD, Balakrishnan N, Joseph B and Gupta VK. CO Oxidation by Cobalt Oxide: An Experimental Study on the Relationship between Nanoparticle Size and Reaction Kinetics. Austin Chem Eng. 2014;1(2): 1008.

surface reacts with molecular oxygen to form an intermediate OCO and O on the surface [18]. OCO intermediate then desorbs to form CO_2 in the gaseous phase. DFT calculations on the activation barriers for these reactions suggest that Mechanisms I and II have much higher activation barriers compared to Mechanism III suggesting this as the most likely route for the oxidation [20]. In this study, Mechanism III is explored in more detail. Mechanism III is a two-step process with two activation barriers one for the formation of the OCO intermediate and a second barrier for the formation of CO_2.

Methods

Synthesis of a model CoO/SiO_2 colloidal catalyst

Surface modified SiO_2

Colloidal non-porous SiO_2 substrates were used to support CoO nanoparticle catalysts. In the fundamental study reported here, non-porous support are advantageous because porous catalyst support structures become a barrier for the transfer of reactant/product species from the catalyst surface into the gas phase [21]. Since repeated adsorption and desorption of radicals may take place within the pores, the use of a porous supported catalyst becomes more complex and not ideal for fundamental studies of catalytic reactions such as one studied here. Sub-micron non-porous spherical SiO_2 colloids were synthesized using a modified Stöber process [22]. The synthesis procedure is well documented in literature. Typically, 3.14 ml of 28-30 wt% NH_4OH was added to an ethanol-water mixture and equilibrated for 30 min. An aliquot of 6ml TEOS was added and stirred for 6 hours at room temperature to yield monodisperse sub-micron SiO_2 particles. The NH_4OH in solution helps to control the charge of the SiO_2 colloids. The SiO_2 colloid solution was purified by centrifuging the solution at 7,000 rpm for 30 minutes and the resulting residue was washed 3 times with water. The particles were dried overnight under vacuum at room temperature.

Cobalt oxide nanoparticles were immobilized by tailoring the surface of Stöber SiO_2 with favorable chemical functional groups. Surface –OH groups on Stöber SiO_2 were covalently modified by methacryloxypropyltrimethoxysilane (MPS), a small molecule ligand that contains a carboxyl (–C=O) functional group.MPS was added to a colloidal (6 wt %) Stöber SiO_2 solution dispersed in 70% ethanol in water and stirred for approximately 12 hours. The solution was held at 80°C for 1 hour to promote covalent bonding of the organosilane molecules to the surface of the SiO_2 colloids [23,24]. The amount of MPS ligand added was ~50% in excess of that required for full coverage, which was estimated based on 25 $Å^2$ per molecule of MPS on the SiO_2 surface. The colloidal solution was purified in a similar manner to Stöber SiO_2 colloids. Colloidal suspensions of surface modified SiO_2 in toluene were prepared by dispersing ~1mg of solids with 10ml of toluene for further use.

Size control during synthesis of CoO catalysts

The size of cobalt nanoparticles was tuned by varying the ratio between the amount of dicobalt octacarbonyl and AOT surfactant in the recipe for CoO synthesis [25-27]. First, a solution of 30 ml toluene and 150 mg of AOT was refluxed at 110°C under a nitrogen atmosphere. Separately, a 10 ml solution containing 1.2 gm dissolved dicobalt octacarbonyl in toluene was prepared. A 200 µL aliquot of cobalt precursor solution was injected rapidly into the hot surfactant solution. After 2 hours, ~1ml of this solution was withdrawn for mixing with the surface modified SiO_2 colloidal solution. An additional 800 µL of cobalt carbonyl precursor was added into the hot refluxing toluene solution and the reaction was continued for an additional 1 hour and a new sample was withdrawn at this point. Thereafter, at every 1 hour interval, additional 1 ml of cobalt precursor solution was injected into the hot solution. Two more samples were collected after a total of 6ml and 10ml of cobalt precursor solution were added to the hot solution. Each cobalt solution that was withdrawn was mixed with ~1gm of surface modified SiO_2 colloidal solution dispersed in toluene. The nanoparticles of CoO were immobilized on the surface of the SiO_2 support via self-assembly and after a few hours, CoO/SiO_2 nanocomposites settled to the bottom, whereas the excess CoO nanoparticles remained in the supernatant. The CoO/SiO_2 residue was separated by decantation. Purification cycles of settling and decantation were repeated 2-3 times by dispersing the residue with pure toluene after every decantation step. The final product was dried at 60-70°C in the vacuum oven for ~1day. As indicated by the above procedure, the samples of CoO of different sizes supported on surface modified SiO_2 were obtained by adjusting the molar ratio (R) of cobalt precursor to surfactant. The approximate R values in used in this study were 0.2, 1, 6 and 10.

Temperature programmed reaction

CO oxidation reaction was studied using AABSPEC #2000A module on a Bio-RAD Excalibur FTS3000 IR instrument. AABSPEC #2000A is a stainless steel reactor equipped with zinc selenide (ZnSe) windows for in-situ FTIR spectroscopy measurements. CoO/SiO_2 nanocomposites were pressed into pellets and placed along the IR beam on a programmable hot finger inserted into the FTIR reactor. Actual temperatures were monitored by an external thermocouple. After placing the catalyst, the chamber was preheated to 150°C for 30min under a 30 sccm N_2 flow to remove any water vapor and then cooled back to room temperature. A gas mixture of CO (10 sccm) and compressed dry air (20 sccm) were introduced using mass flow controllers (approximate ratio of 2.4 for CO to oxygen). Both inlet and outlet valves were closed after 10-15 min of steady flow of gases. A new background signal was collected against which further spectra were compared. Temperature programmed reactions were carried out by increasing the temperature from room temperature to 475°C at a constant heating ramps set at 10, 7.5, 4.5 and 2°C/min. FTIR spectra were collected in transmission mode at regular intervals of time during the temperature programmed reaction. For 10°C/min runs, pure catalyst samples were pressed into ~0.1 mg pellets. In order to get better signal-to-noise ratio, for 7.5, 4.5 and 2°C/min runs, samples were diluted with KBr thereby increasing the transmittance of IR signal.

Material characterization

Electron microscopy measurements were performed on a FEI Morgagni 268D and TECNAI F20 for low resolution and high resolution imaging of CoO/SiO_2 colloids. Samples were prepared by drying a drop of the colloidal solution on a carbon-support film TEM grid (Electron Microscopy Sciences, PA). Hydrodynamic diameter and polydispersity of particles were estimated from dynamic light scattering (DLS) technique using a Nano-S Zetasizer (Malvern). A Philips X'pert materials research diffractometer was used to analyze the crystal structure of the cobalt catalyst nanoparticles.

Results and Discussion

Hydrodynamic size of CoO nanoparticles were approximately 1, 2, 6 and 14nm for different samples by DLS measurements as shown in Figure 1. Figures 2 a,b & c depict TEM images of samples of CoO/SiO_2 samples with CoO average sizes 14, 6 and 2nm supported on SiO_2 colloids. Aggregation of larger CoO nanoparticles was observed that was caused due to the low surfactant concentration. The crystallinity of unsupported CoO nanoparticles prepared using decomposition technique was studied using XRD as shown in Figure 2d. The peak positions were identical in all the samples with different CoO sizes. XRD patterns obtained from previous reports on the synthesis of CoO [27] and a comparison of X-ray diffraction patterns with previous reports suggests that the oxide synthesized from our experiments was CoO in contrast to the other commonly synthesized oxide, Co_3O_4 [28-30].

When CO was introduced into the reactor during the in-situ FTIR studies, bands at 2058, 2140 and 2170 cm^{-1} were observed as shown in Figure 3. The peak at 2058 cm^{-1} corresponds to the adsorption of CO gas on CoO surface [31] and the vibrational frequencies of CO in bulk gaseous phase were seen at 2140 cm^{-1} and 2170 cm^{-1}. The dynamic changes in the 2058 cm^{-1} peak during the temperature programmed reaction and the evolution of CO_2 shown by the appearance of two new bands of 2350 cm^{-1} and 2342 cm^{-1} were used to measure activation energies experimentally. Figure 4 depicts the FTIR spectra collected for composites with 6 nm CoO supported on SiO_2during 10^{O}C/min heating rate. The adsorbed CO and the bulk CO gas peaks 2058 cm^{-1}, 2140 and 2170 cm^{-1} show a decreasing trend with an increase in temperature. The 2058 cm^{-1} peak height was monitored as a function of temperature.

It was found that the peak height decreased as temperature was raised and began to plateau at a particular temperature T′ as depicted in the Figure 5 for different CoO sizes. This plateau-onset temperature T′ and the corresponding heating rates, ψ were used to calculate the activation energy required for the step where adsorbed CO transforms to an intermediate structure. This step where CO_{ads} peak disappears can be attributed to the first step in the Mechanism III. In-situ experiments were used to monitor the disappearance of CO_{ads} peak during the course of the temperature programmed reaction. The CO_{ads} peak suggests that CO_{ads} changes to an intermediate OCO.

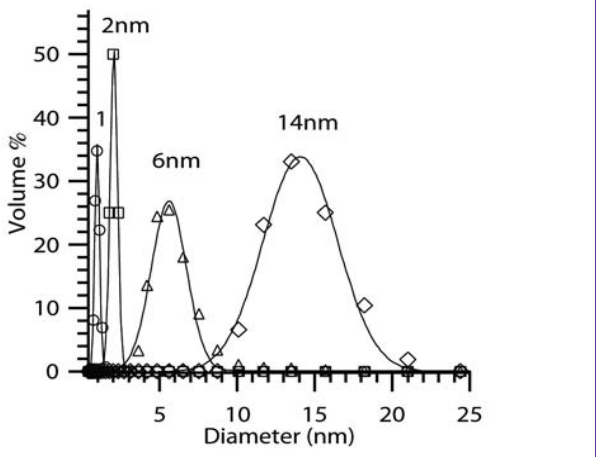

Figure 1: Size distribution of of CoO nanoparticles using DLS technique.

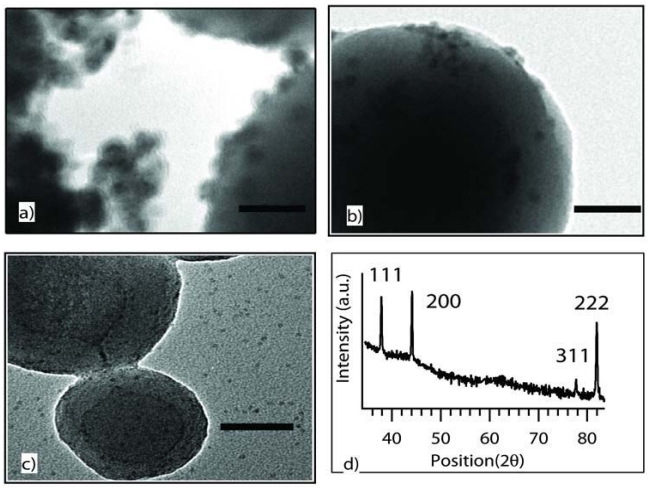

Figure 2: TEM images of supported CoO nanoparticles with size a) 14 nm, b) 6 nm and c) 2 nm. d) XRD of unsupported CoO nanoparticles. All scale bars in a-c are 50 nm

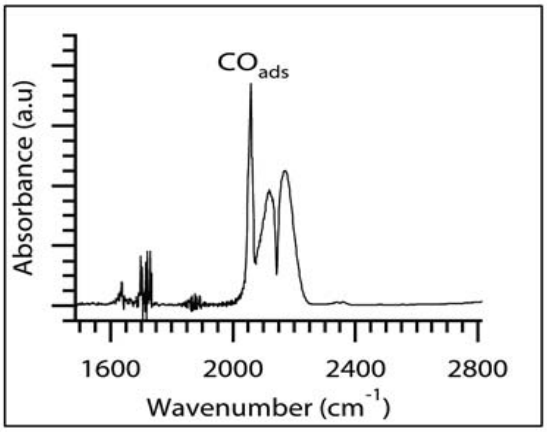

Figure 3: FTIR spectrum collected when CO and air was introduced into the reactor

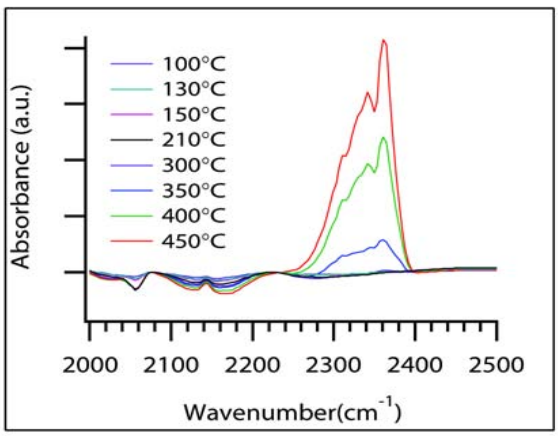

Figure 4. FTIR spectra collected at various intervals of time during a 10°C/min temperature ramp.

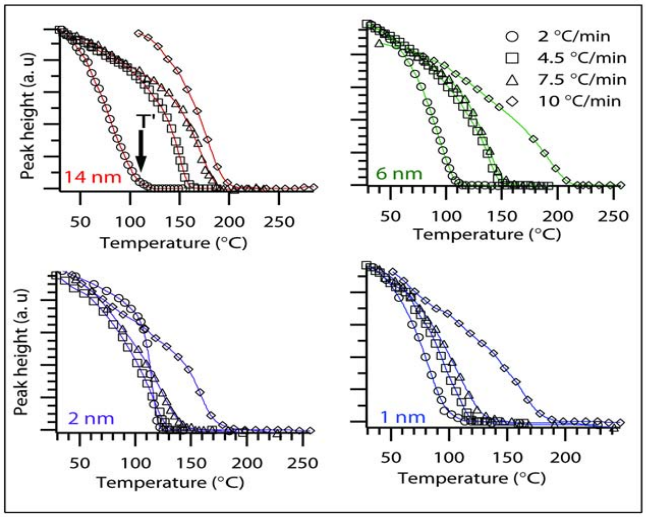

Figure 5: The peak height of 2058 cm^{-1} band recorded during at various heating rates for different samples.

The experimental procedure to measure activation energy for step-1 was similar to the calculations in previous reports on H_2-temperature programmed reduction studies [32-34]. A model equation originally developed by Kissinger [35] and further extended by others [32,34] uses the Arrhenius equation to find activation energies from temperature programmed profiles. The slopes from Figure 6 are used for E_{step-1} calculations. For composites with 1 and 2nm sized CoO nanoparticles, the T´ values obtained from the slowest heating rate, i.e., 2°C/min were not included in the slope measurements due to large deviation from linearity. A plausible reason for the deviation can be cobalt surface reconstruction during a prolonged exposure to CO gas or aggregation of smaller nanoparticles into bigger sized particles. Surface reconstruction behavior of a metal surface such as cobalt metal has been observed in the presence of adsorbing CO gas [36,37]. Activation energy for CO_2 desorption was also calculated. The plot obtained by measuring the concentrations of CO_2 generated for samples of different CoO sizes during the 10°C/min ramp rate is shown in Figure 7. The data points were fitted to an empirical rate equation available in literature [38,39] for a batch mode differential reaction to estimate the activation energies of the catalytic step.

Figure 8 summarizes the relationship between CoO nanoparticle size and activation energies for the two steps measured experimentally. The x-axis error bars depict the variation in nanoparticle sizes which was obtained from the widths of size peaks measured using DLS technique. The y-axes error bars are generated from the deviation values of activation energies when experimental observations were fitted to the derived Arrhenius equation. We can see from experimental measurements that both activation energy values for step-1 and step-2 increase as nanoparticle size increase. The activation barrier for step-1 is low compared to that of step-2. We believe that the reaction is initiated by the reaction between adsorbed CO and O2 on the surface to form the OCO intermediate. The desorption of OCO to form gaseous CO2 apparently has the higher activation barrier and therefore becomes the rate determining step. We plan to examine this in more detail using DFT calculations in the future.

Prior studies in the literature have reported that the lattice

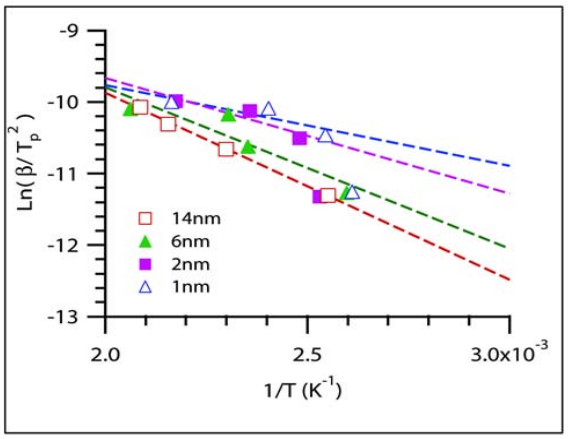

Figure 6: Kissinger plot to find Estep-1 from slope -E/R

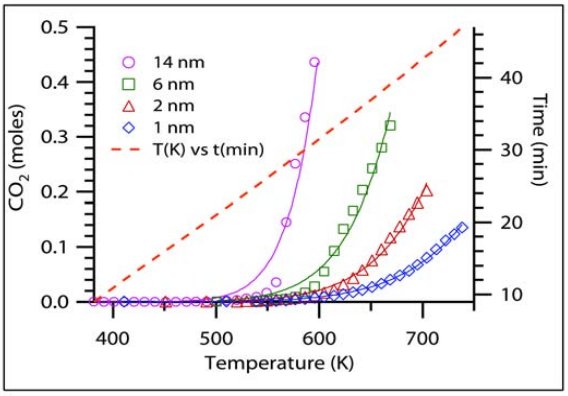

Figure 7: CO2 profile for nanocomposites with different CoO sizes during the heating ramp of10°C/min.

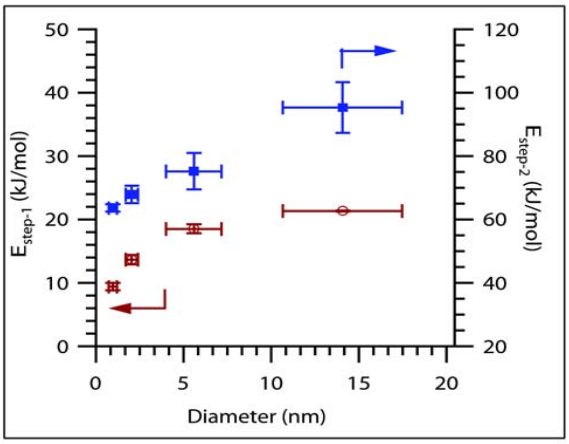

Figure 8: Activation energies of step-1 and step-2 plotted as a function of CoO nanoparticle size.

constant decreases as the size decreases [40-42]. Other studies indicate that even small changes in lattice constant can significantly affect the binding energies of surface species [43]. This suggests that the decrease in activation energy with decrease in size may be attributed to changes in the lattice structure.

Other effects that can influence the reaction rates are total number

of active sites which will depend on the exposed facets, the step edges and corner atoms present on the surface of the catalyst all of which change with the size. A similar phenomenon has been observed in previous studies where metal flat surfaces [44] or metal clusters of Fe with 55 atoms [45] were used to compute the difference in energy barriers on metal sites with different coordination numbers.

Conclusions

CO oxidation over CoO nanoparticles is significantly influenced by the size of the catalyst particles. The experimental results are in agreement with a two-step reaction mechanism in which CO first reacts on the surface to form an OCO intermediate followed by dissociation to form CO_2 in the gas phase. The activation energy barrier for the first step is smaller than the second step. Both activation energies increase with the catalyst particle size suggesting that smaller particles are more active for CO oxidation. One plausible explanation for the size effect is the decrease in lattice spacing as size decreases. Other possible causes include an increase in the number of atoms with lower coordination number and increase in number of corner and step edges as the particle size decreases. Developing protocols for a systematic analysis of role of nanoparticle size of relatively unexplored metals can help in the development of the next generation catalysts.

Author Contributions

The manuscript was written through contributions of all authors. All authors have given approval to the final version of the manuscript.

Funding Sources

University of South Florida, Florida Energy Systems Consortium (FESC) Computational Cluster Grant under MRI Award 072287, NSF Curriculum Reform Grant Award 0530444.

Acknowledgment

We acknowledge financial support from University of South Florida, Florida Energy Systems Consortium (FESC), Computational Cluster Grant under MRI Award 072287, and the NSF Curriculum Reform Grant Award 0530444. Resources at the USF research computing and Extreme Science and Engineering Discovery Environment (XSEDE) are also acknowledged.

References

1. Janssens T, Clausen B, Hvolbæk B, Falsig H, Christensen C, Bligaard T, et al. Insights into the reactivity of supported Au nanoparticles: combining theory and experiments. Topics in Catalysis. 2007; 44: 15-26.
2. Dahl S, Logadottir A, Egeberg RC, Larsen JH, Chorkendorff I, Törnqvist E, et al. Role of Steps in N2 Activation on Ru(0001). Physical Review Letters. 1999; 83: 1814-1817.
3. Daté M, Haruta M, Catal J. 2001; 201: 221-224.
4. Haruta M, Tsubota S, Kobayashi T, Kageyama H, Genet MJ, Delmon B. Low-temperature oxidation of CO over gold supported on TiO_2, -$F_{e2}O_3$, and Co_3O_4. J. Catal. 1993; 144: 175-192.
5. Herzing AA, Kiely CJ, Carley AF, Landon P, Hutchings GJ. Identification of active gold nanoclusters on iron oxide supports for CO oxidation. See comment in PubMed Commons below Science. 2008; 321: 1331-1335.
6. Oh SH, Sinkevitch RM. Carbon Monoxide Removal from Hydrogen-Rich Fuel Cell Feedstreams by Selective Catalytic Oxidation. J Catal. 1993; 142: 254-262.
7. Schubert MM, Hackenberg S, van Veen AC, Muhler M, Plzak V, Behm RJ. CO Oxidation over Supported Gold Catalyst - "Inert" and "Active" Support Materials and Their Role for the Oxygen Supply during Reaction. J. Catal. 2001; 197: 113-122.
8. Boudart M, Rumpf F. The catalytic oxidation of CO and structure insensitivity. React. Kinet. Catal L. 1987; 35: 95-105.
9. Grass ME, Zhang Y, Butcher DR, Park JY, Li Y, Bluhm H, et al. A reactive oxide overlayer on rhodium nanoparticles during CO oxidation and its size dependence studied by in situ ambient-pressure X-ray photoelectron spectroscopy. See comment in PubMed Commons below Angew Chem Int Ed Engl. 2008; 47: 8893-8896.
10. Haruta M. When gold is not noble: catalysis by nanoparticles. See comment in PubMed Commons below Chem Rec. 2003; 3: 75-87.
11. Joo SH, Park JY, Renzas JR, Butcher DR, Huang W, Somorjai GA, et al. Size effect of ruthenium nanoparticles in catalytic carbon monoxide oxidation. See comment in PubMed Commons below Nano Lett. 2010; 10: 2709-2713.
12. McCarthy E, Zahradnik J, Kuczynski GC, Carberry JJ. Some unique aspects of CO oxidation on supported. J. catal. 1975; 39: 29-35.
13. Overbury SH, Schwartz V, Mullins DR, Yan W, Dai S. "Evaluation of the Au size effect: CO oxidation catalyzed by Au/TiO2." J. Catal. 2006; 241: 56-65.
14. Valden M, Lai X, Goodman DW. Onset of catalytic activity of gold clusters on titania with the appearance of nonmetallic properties See comment in PubMed Commons below Science. 1998; 281: 1647-1650.
15. Xie X, Li Y, Liu ZQ, Haruta M, Shen W. Low-temperature oxidation of CO catalysed by Co(3)O(4) nanorods. See comment in PubMed Commons below Nature. 2009; 458: 746-749.
16. Bennett CO. Experiments and Processes in the Transient Regime for Heterogeneous Catalysis. In: Haag WO, Gates BC, Helmut K, Editors. Advances in Catalysis, Academic Press. 1999; 44: 329-416.
17. Kobayashi H, kobayashi M. Transient response method in heterogenous catalysis. Catal. Rev. Sci. Eng. 1974; 10: 139-176.
18. Derekaya FB, Guldur C. Int. J. Chem. Reactor Eng. 2010; 8: 1-18.
19. Gong XQ, Raval R, Hu P. General insight into CO oxidation: a density functional theory study of the reaction mechanism on platinum oxides. See comment in PubMed Commons below Phys Rev Lett. 2004; 93: 106104.
20. Balakrishnan N. Theoretical Studies of Co Based Catalysts on CO Hydrogenation and Oxidation. Chemical and Biomedical Engineering, University of South Florida, Tampa. 2013.
21. Couwenberg PM, Chen Q, Marin GB. Kinetics of a Gas-Phase Chain Reaction Catalyzed by a Solid: The Oxidative Coupling of Methane over Li-MgO-Based Catalysts. Ind. Eng. Chem. Res. 1996; 35: 3999-4011.
22. Stoeber W, Fink A, Bohn E. Controlled growth of monodisperse silica spheres in the micron size range. J. Colloid Interface Sci. 1968; 26: 62-69.
23. Reculusa S, Mingotaud C, Bourgeat-Lami E, Duguet E, Ravaine S. Synthesis of Daisy-Shaped and Multipod-like Silica/Polystyrene Nanocomposites. Nano Lett. 2004; 4: 1677-1682.
24. Westcott SL, Oldenburg SJ, Lee TR, Halas NJ. Formation and Adsorption of Clusters of Gold Nanoparticles onto Functionalized Silica Nanoparticle Surfaces. Langmuir. 1998; 14: 5396-5401.
25. Huber DL, Venturini El, Martin JE, Provencio PP, Patel RJ. Synthesis of highly magnetic iron nanoparticles suitable for field structuring using a β-diketone Surfactant. Magn J. Magn. Mater. 2004; 278: 311-316.
26. Papirer E, Horny P, Balard H, Anthore R, Petipas C, Martinet A. The preparation of a ferrofluid by decomposition of dicobalt octacarbonyl: I. Experimental Parameters. J. Colloid Interface Sci. 1983; 94: 207-219.
27. Yin JS, Wang ZL. Ordered Self-Assembling of Tetrahedral Oxide Nanocrystals. Phys. Rev. Lett. 1997; 79: 2570-2573.
28. Yu Y, Ji G, Cao J, Liu J, Zheng M. Facile synthesis, characterization and electrochemical properties of cuspate deltoid CoO crystallites. J. Alloys Compd. 2009; 471: 268-271.

29. Zhang L, Xue D. Preparation and magnetic properties of pure CoO nanoparticles. J. Mater. Sci. Lett. 2002; 21: 1931-1933.

30. Zhuo L, Ge J, Cao L, Tang B. Solvothermal Synthesis of CoO, Co3O4, Ni(OH)2 and Mg(OH)2 Nanotubes. Cryst. Growth Des. 2008; 9: 1-6.

31. Kadinov G, Bonev C, Todorova S, Palazov A. IR spectroscopy study of CO adsorption and of the interaction between CO and hydrogen on alumina-supported cobalt. J. Chem. Soc., Faraday Trans. 1998; 94: 3027-3031.

32. Gentry SJ, Hurst NW, Jones A. Temperature programmed reduction of copper ions in zeolites. J. Chem. Soc., Faraday Trans. 1979; 75: 1688-1699.

33. Lin H-Y, Chen Y-W, Li C. The Mechanism of reduction of iron oxide by hydrogen. Thermochim. Acta. 2003; 400: 61-67.

34. Wimmers OJ, Arnoldy P, Moulijn JA. Determination of the reduction mechanism by temperature-programmed reduction: application to small iron oxide (Fe2O3) particles. J. Phys. Chem. 1986; 90: 1331-1337.

35. Kissinger HE. Reaction Kinetics in Differential Thermal Analysis. Anal. Chem. 1957; 29: 1702-1706.

36. Ciobîca IM, van Santen RA, van Berge PJ, van de, Loosdrecht J. Adsorbate induced reconstruction of cobalt surfaces. Surf. Sci. 2008; 602: 17-27.

37. Hendriksen BL, Ackermann MD, van Rijn R, Stoltz D, Popa I, Balmes O, et al. The role of steps in surface catalysis and reaction oscillations. See comment in PubMed Commons below Nat Chem. 2010; 2: 730-734.

38. Coats AW, Redfern JP. Kinetic Parameters from Thermogravimetric Data. Nature. 1964; 201: 68-69.

39. Ortiz MI, Romero A, Irabien A. Integral kinetic analysis from temperature programmed reaction data: alkaline hydrolysis of ethyl acetate as test reaction. Thermochim Acta. 1989; 141: 169-180.

40. Qi WH, Wang MP. Size and shape dependent lattice parameters of metallic nanoparticles. J. Nanopart. Res. 2005; 7: 51-57.

41. Viñes F, Illas F, Neyman KM. Density functional calculations of Pd nanoparticles using a plane-wave method. See comment in PubMed Commons below J Phys Chem A. 2008; 112: 8911-8915.

42. Wang L, Roudgar A, Eikerling M. Ab Initio Study of Stability and Site-Specific Oxygen Adsorption Energies of Pt Nanoparticles. J. Phys. Chem. C. 2009; 113: 17989-17996.

43. Zhao R, Lee SJ, Son IH, Lee H, Soon A. First-Principles Based Phenomenological Study of Ni Nanocubes: The effects of Nanostructuring on Carbon Poisoning of Ni(001) Nanofacets. Appl. Surf. Sci. 2013; 265: 339-345.

44. Ge Q, Neurock M. Adsorption and activation of CO over flat and stepped Co surfaces: a first principles analysis. See comment in PubMed Commons below J Phys Chem B. 2006; 110: 15368-15380.

45. Lanzani G, Nasibulin AG, Laasonen K, Kauppinen EI. CO Disproportionation on a Nanosized Iron Cluster. J Phys Chem C. 2009; 113: 12939-12942.

Austin Chem Eng - Volume 1 Issue 2 - 2014
ISSN : 2381-8905 | www.austinpublishinggroup.com

Citation: Mankidy BD, Balakrishnan N, Joseph B and Gupta VK. CO Oxidation by Cobalt Oxide: An Experimental Study on the Relationship between Nanoparticle Size and Reaction Kinetics. Austin Chem Eng. 2014;1(2): 1008.